Supplementary Information

Materials and Methods

Pump-CTD and nutrient measurements

The pump-CTD system had an approximate water flow of 1.5 l min^{-1} in a FALMAT-hose cable with an outer diameter of 18 and an inner diameter of 6 mm. The pump tube was directed into the lab and split into a nutrient and a gas line. Measurements with custom-made STOX-sensors (Unisense, Denmark) revealed a background concentration of 25 nmol/l oxygen originating from the pump-CTD system. Pumping volume was constantly controlled via precision flow-through devices, and delay time between pump inlet and sample outlet was continuously calculated and converted to sampling depth. All samples were measured during lowering of the system with a speed of 1 cm s^{-1} (further details in the cruise report: DOI: 10.2323/cr_msm33). To construct depth profiles from successive casts, data were aligned according to density; for all these profiles the depths showing the respective densities during the first cast were used.

For continuous nutrient measurements in the outflow of the pump-CTD, the auto-analyzer was connected to the water outlet of the pump-CTD system. The injection syringe of the auto-sampler dipped directly into the core pool of the outflowing water and thereby avoided any contact of the samples with laboratory air prior to analysis. This procedure considerably reduced contamination, particularly of ammonium. Sampling time was set to 26 s and washing time to 7 s. As the lowering speed of the pump-CTD was set to 1 cm/s, the vertical resolution of sampling was 33 cm throughout the observed water column, of which 26 cm were included in successive analytical pulses and thereby integrated, and 7 cm were lost due to rinsing and blank measurements between the injections.

Nucleic acid extractions

For metagenome analysis 6 l of water were filtered on Sterivex-GV 0.22 µm, PVDF. DNA from frozen Sterivex-filters was extracted using a QIAmp DNA Mini kit (Qiagen, Hilden, Germany) after removing the filter from the plastic support. For physical cell disruption, the filter pieces were added to a tube containing lysis buffer and low-binding zirconium beads (200 µm, OPS diagnostics, Lebanon, NJ, USA) and vortexed for 5 min before proceeding with the manufacturer's instructions. The extracted DNA was sent for library preparation (BS80: Illumina TruSeq PCR free library; BS90, BS102, BS115: Rubicon Thruplex library prep) and Illumina HiSeq sequencing to the SciLife Lab (Stockholm, Sweden). For metatranscriptomic analyses from six selected depths, 1.5 l of fixed water samples from the AFIS system were filtered on 0.2 µm polycarbonate filter and stored at -80 °C. RNA from frozen filters was extracted as described elsewhere (1). For downstream absolute quantification of RNA transcripts, standards were added to the lysis buffer before the start of RNA extraction (2). Due to a lysis buffer spill during the extraction of the sample from 111 m water depth, absolute transcript numbers will be slightly overestimated in this sample. DNA leftovers in the RNA extracts were removed using a Turbo DNA-free Kit (Thermo-Fisher Scientific, Waltham, MA USA) and subsequently concentrated and purified using the RNA Clean & Concentrator™-5 Kit (Zymo Research, Irvine, CA, USA). Because positive PCR amplifications with the 16S rRNA specific primers Com1f/Comr2r-Ph (3) indicated the presence of DNA traces in the RNA extracts, DNase digestion and subsequent purification was repeated as described above. The purified RNA was sent to Fasteris (Plan-les-Ouates, Switzerland) for Illumina-HiSeq sequencing after rRNA depletion with the RiboZero kit for bacteria (Epicentre, Madison, WI, USA). Library preparation for single reads was performed using the TruSeq stranded mRNA kit (Illumina, San Diego, CA, USA).

Bioinformatic processing of Illumina sequence data

Paired Illumina reads from 4 individual metagenome libraries were screened for rRNA-reads using SortMeRNA 1.9 on the default rRNA-databases provided by the program. Remaining non-rRNA-reads were adaptor-clipped using mira 4.0.2 (4) and quality clipped using sickle 1.33 (default settings) (5). Remaining intact read pairs from all four libraries were combined and assembled using idba_ud 1.1.1 (--mink 25 --maxk 97 --step 18) (6). Contigs shorter than 200 nt were discarded. Gene calling was performed using Prodigal's meta-procedure (v2.6.1) (7). CDSs from the Prodigal output were functionally and taxonomically annotated using NCBI's blastp (8) against KEGG and NCBI's NR. Genes of special interest were identified using IHAT as described by Temperton et al. (2011) (9). Single-end metatranscriptome reads were also adaptor- and quality clipped as described above and mapped onto the previously generated metagenome using bowtie2 2.2.4 (10) with the very-sensitive settings. Mapped reads were summarized using featureCounts 1.4.6 (11), requiring a minimum of 20 overlapped bases to assign a read to a feature. The number of reads coding for internal standards of the metatranscriptome data were determined in every sample by a LAST search (12) of the non-protein coding reads against a database containing sequence information of the internal standards as well as representative rRNA and tRNA sequences (cutoff score: 500). The number of transcripts l^{-1} for Ppk1, Ppk2 and Ppx was estimated as detailed in Satinsky et al. (2013) (2). In short, knowledge of the sequence of internal standards and the exact amount of ng internal standard RNA added allowed us to calculate the number of RNA internal standard molecules that were added to each RNA extractions. The recovery rate of the standard molecules in the sequencing data reads can be used to estimate fraction of RNA molecules in the sample that were sequenced and deduce from this value the absolute number of transcripts that were in the filtered water volume.

Analysis of bacterial community composition, probe design and catalysed reporter deposition-fluorescence in situ hybridization

Of the Phenol/Chloroform extracted DNA/RNA mixture, DNA was digested using the Turbo DNA free kit (Ambion). The RNA was transcribed in cDNA utilizing the iScript Select cDNA synthesis kit (Bio-Rad Laboratories GmbH; Munich, Germany). After 16S rRNA gene amplification the amplicons were purified using Agencourt© AMPure ® XP (Becker Coulter) and sent for sequencing. The resulting sequences were analyzed using SILVA_NGS (Glöckner et al., 2017) with the settings Min. Align. Identity: 50%; Min. Align. Score: 40; Min. Sequence Quality 30%; Min Length: 200, Max Ambiguties: 2%, Min OTU Identity: 97%, Min. Smilarity: 93%. SILVA NGS performs additional quality checks according to the SINA-based alignments (Pruesse et al., 2012) with a curated seed database in which PCR artifacts or non-SSU reads are excluded. The longest read serves as a reference for the taxonomic classification in a BLAST (version 2.2.28+) search against the SILVA SSURef dataset. The classification of the reference sequence of a cluster (97% sequence identity) is then mapped to all members of the respective cluster and to their replicates. Best BLAST hits were only accepted if they had a (sequence identity + alignment coverage)/2 $\geq$ 93 or otherwise defined as unclassified.

CARD-FISH was carried out using the horseradish-peroxidase-labeled probe MaCo983. The competitor probe MaCo983 without horseradish-peroxidase label was applied in parallel. For signal amplification, tyramide labeled with the fluorescent dye carboxyfluoresceine was incubated for 30 min at 37 °C. The filters were embedded in a Citifluor/Vetashield mix (5: 1) containing 4,6-diamidino-2-phenylindole (1 μg ml^{-1} final concentration). Images were acquired using a 100× Plan-Apochromat objective (Zeiss) and the Zeiss multi-band filter set 62HE.

Scanning electron microscopy (SEM) and energy dispersive x-ray micro analysis (EDX)

Suspended particulate matter in 1 l seawater samples taken from the CTD rosette bottle was filtered on 0.4 µm polycarbonate filters (Millipore) and rinsed with 50 ml purified water to remove salt. After drying at 40 °C for 48 h, the filters were covered (vacuum sputter) with elemental carbon for electrical conductivity. Analysis of carbon in these samples is thus not possible, but this technique is optimal for analyzing all other elements. The identification of minerals after automated particle element analyses is based on boundary values of characteristic elements. These boundary values were defined by analyses of standard minerals and adjusted by analyses of samples with known mineral composition. However, besides the additional information about the detected minerals or particle groups, the whole data set for each sample was analyzed with a statistic software (xls; DataDesk) to verify the detected clusters of particles in a "multi element space". Using this method, we were able to characterize the general mineral and particle group composition of the samples and to search for P in different binding forms.

Modeling

In our modeling approach the differential equation for diffusive transport (Fick's second law):

(1) $\delta c / \delta t = D \cdot \delta^2 c / \delta x^2$

(D = diffusion coefficient, c = concentration, t = time; x = distance-coordinate), is solved by using the explicit numerical solution:

(2) $C_{PO_4(x,t+\Delta t)} = C_{PO_4(x,t)} + \Delta t \cdot D_x \cdot (C_{PO_4(x+\Delta x,t)} - 2 \cdot C_{PO_4(x,t)} + C_{PO_4(x-\Delta x,t)}) / \Delta x^2 + \Delta t \cdot Prod_x$

where C_{PO_4} is the concentration of phosphate at a given place x and time t, D_x is the diapycnal diffusivity at the depth x, as determined by Gregg and Yakushev (13), x is the depth and $Prod_x$ is a change of concentration at a given depth per time step, caused by the release of phosphate from the particulate phosphorus pool, or visa verse a negative release is an incorporation into the particulate phosphorus pool. When the calculation of all concentrations of a time step is

completed, the next time step starts with the final concentrations of the preceding time step. By this approach, the concentration of phosphate with depth is calculated in cell E12-E172 for depths between 80 and 120 m (cell C12-C172) with a Δx of 0.25 m (cell B12). Under starting conditions (cell F12-F172), when the model is reset with the switch in cell B10, phosphate increases linearly with depth. This starting condition is without influence on the concentrations in a final steady state. Only the concentration of the first cell (E12) and the rates with which phosphate is released from the particulate pool or incorporated into it (cells G12-G172) determine the final phosphate concentration. These latter rates were manually adjusted until they resulted, under steady state, in a profile similar to the measured one. Steady state is reached after approximately 3 years (cell B26).

The modelled concentrations of particulate phosphorus originate only from the fluxes into and out of the dissolved pool. These fluxes are adjusted to produce the same shape of the phosphate profile as observed in nature. According to the depth-dependent rates $Prod_x$, with which phosphate is released from or incorporated into the particulate pool (cells G12-G172), the concentration of *PartP* (cells H12-H172) changes with each time step, which is expressed by:

(3) $$PartP_{(x,t+\Delta t)} = PartP_{(x,t)} - \Delta t \cdot Prod_{(x)}$$

Screenshot of the model after reset:

EXPLICIT numerical solution for advective, dispersive/diffusive transport and simple reactions (as described by H.D. Schulz, in Chapter 15: Conceptual Models and Computer Models. In: Marine Geochemistry Eds. H.

How to use this spreadsheet:

1. Set your EXCEL via Tools – Options – Calculation to Calculation = Manual, to Iteration = 1 and to Maximum Iterations = 1000
2. Now each pressing of the F9 key is one time step of the explicit numerical solution
3. An input of '1' into position B10 and pressing F9 resets the spreadsheet to the start conditions
4. An input of '0' into position B10 and repeated pressing F9 performs the model calculation. In B26 the time since the model started is given in years
5. Note the two diagrams towards the right with A)measured phosphate and particulate P profiles (red) and profiles resulting from the model (green) and B) flux rates used for production and consumption in the modes

		x	D	C PO4	C PO4_start	Prod	part P	part P start
Reset = 1	1	(m)	m2/s	(mmol/m3)	(mmol/m3)	mmol/m3*s	(mmol/m3)	(mmol/m3)
delta_x =	0.25	80.00	4.00E-06	1.40	1.40	0.00E+00	0.02	0.02
dt_max =	833	80.25	3.98E-06	1.43	1.43	0.00E+00	0.02	0.02
delta_t =	800	80.50	3.96E-06	1.45	1.45	0.00E+00	0.02	0.02
		80.75	3.94E-06	1.48	1.48	0.00E+00	0.02	0.02
		81.00	3.93E-06	1.51	1.51	0.00E+00	0.02	0.02
sink_vel (m/s) =	0.000075	81.25	3.91E-06	1.53	1.53	0.00E+00	0.02	0.02
sink_vel (m/d) =	6.5	81.50	3.89E-06	1.56	1.56	0.00E+00	0.02	0.02
		81.75	3.87E-06	1.59	1.59	0.00E+00	0.02	0.02
		82.00	3.85E-06	1.62	1.62	0.00E+00	0.02	0.02
TIME COUNT:		82.25	3.83E-06	1.64	1.64	0.00E+00	0.02	0.02
		82.50	3.81E-06	1.67	1.67	0.00E+00	0.02	0.02
t_total(s) =	0	82.75	3.79E-06	1.70	1.70	0.00E+00	0.02	0.02
t_total(h) =	0.00	83.00	3.78E-06	1.72	1.72	0.00E+00	0.02	0.02
t_total(d) =	0.00	83.25	3.76E-06	1.75	1.75	0.00E+00	0.02	0.02
t_total(yrs) =	0.0	83.50	3.74E-06	1.78	1.78	0.00E+00	0.02	0.02
		83.75	3.72E-06	1.80	1.80	0.00E+00	0.02	0.02
		84.00	3.70E-06	1.83	1.83	0.00E+00	0.02	0.02
		84.25	3.68E-06	1.86	1.86	0.00E+00	0.02	0.02
		84.50	3.66E-06	1.88	1.88	0.00E+00	0.02	0.02
		84.75	3.64E-06	1.91	1.91	0.00E+00	0.02	0.02
		85.00	3.63E-06	1.94	1.94	0.00E+00	0.02	0.02
		85.25	3.61E-06	1.96	1.96	0.00E+00	0.02	0.02
		85.50	3.59E-06	1.99	1.99	0.00E+00	0.02	0.02
		85.75	3.57E-06	2.02	2.02	0.00E+00	0.02	0.02
		86.00	3.55E-06	2.05	2.05	0.00E+00	0.02	0.02
		86.25	3.53E-06	2.07	2.07	5.45E-08	0.02	0.02
		86.50	3.51E-06	2.10	2.10	5.45E-08	0.02	0.02
		86.75	3.49E-06	2.13	2.13	5.45E-08	0.02	0.02
		87.00	3.48E-06	2.15	2.15	1.42E-07	0.02	0.02
		87.25	3.46E-06	2.18	2.18	1.42E-07	0.02	0.02
		87.50	3.44E-06	2.21	2.21	2.29E-07	0.02	0.02
		87.75	3.42E-06	2.23	2.23	3.27E-07	0.02	0.02
		88.00	3.40E-06	2.26	2.26	4.92E-07	0.02	0.02
		88.25	3.38E-06	2.29	2.29	5.74E-07	0.02	0.02
		88.50	3.36E-06	2.31	2.31	6.05E-07	0.02	0.02
		88.75	3.34E-06	2.34	2.34	6.05E-07	0.02	0.02
		89.00	3.33E-06	2.37	2.37	6.05E-07	0.02	0.02
		89.25	3.31E-06	2.39	2.39	5.74E-07	0.02	0.02
		89.50	3.29E-06	2.42	2.42	4.92E-07	0.02	0.02
		89.75	3.27E-06	2.45	2.45	2.29E-07	0.02	0.02
		90.00	3.25E-06	2.48	2.48	-2.89E-07	0.02	0.02
		90.25	3.23E-06	2.50	2.50	-2.89E-07	0.02	0.02
		90.50	3.21E-06	2.53	2.53	-4.82E-07	0.02	0.02
		90.75	3.19E-06	2.56	2.56	-5.50E-07	0.02	0.02
		91.00	3.18E-06	2.58	2.58	-7.15E-07	0.02	0.02
		91.25	3.16E-06	2.61	2.61	-7.15E-07	0.02	0.02
		91.50	3.14E-06	2.64	2.64	-7.70E-07	0.02	0.02
		91.75	3.12E-06	2.66	2.66	-7.70E-07	0.02	0.02
		92.00	3.10E-06	2.69	2.69	-8.25E-07	0.02	0.02
		92.25	3.08E-06	2.72	2.72	-8.25E-07	0.02	0.02
		92.50	3.06E-06	2.74	2.74	-8.25E-07	0.02	0.02
		92.75	3.04E-06	2.77	2.77	-8.25E-07	0.02	0.02
		93.00	3.03E-06	2.80	2.80	-8.25E-07	0.02	0.02
		93.25	3.01E-06	2.82	2.82	-8.25E-07	0.02	0.02

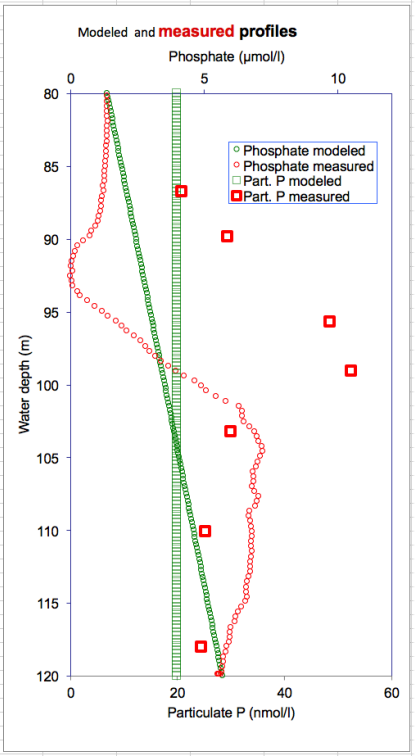

When the model is reset to time zero (as explained in the head of the spreadsheet) the particulate phosphorus pool *PartP* is set to a concentration of 20 nmol l^{-1} at all depths, which is the concentration measured directly above the suboxic zone. Over time the transport of phosphorus from the dissolved into the particulate pool alone, without a removal of particulate phosphorus, would result in *PartP* concentrations orders of magnitude higher than observed in nature. Therefore, the model contains a function, which removes particulate phosphorus by sinking of particles. For this, a certain amount of *PartP* in each cell oh H12-H172 is moved to the cell below with a sinking velocity, *sinkvel* (entered in cell B17 in m s^{-1}) by adding the term:

(4) $$+ (PartP_{(x-\Delta x,t)} \cdot sinkvel \cdot \Delta t / \Delta x - PartP_{(x,t)}) \cdot sinkvel \cdot \Delta t / \Delta x$$

The sinking velocity in the model was adjusted to result in similar particulate phosphorus levels as observed in nature.

Screenshot of the model at steady state after 3 years:

EXPLICIT numerical solution for advective, dispersive/diffusive transport and simple reactions (as described by H.D. Schulz, in Chapter 15: Conceptual Models and Computer Models. In: Marine Geochemistry Eds. H.

How to use this spreadsheet:

1. Set your EXCEL via Tools -- Options -- Calculation to Calculation = Manual, to Iteration = 1 and to Maximum Iterations = 1000
2. Now each pressing of the F9 key is one time step of the explicit numerical solution
3. An input of '1' into position B10 and pressing F9 resets the spreadsheet to the start conditions
4. An input of '0' into position B10 and repeated pressing F9 performs the model calculation. In B26 the time since the model started is given in years
5. Note the two diagrams towards the right with A)measured phosphate and particulate P profiles (red) and profiles resulting from the model (green) and B) flux rates used for production and consumption in the modes

Reset = 1	0	x	D	C PO4	C PO4_start	Prod	part P	part P start
		(m)	m2/s	(mmol/m3)	(mmol/m3)	mmol/m3*s	(mmol/m3)	(mmol/m3)
delta_x =	0.25	80.00	4.00E-06	1.40	1.40	0.00E+00	0.02	0.02
dt_max =	833	80.25	3.98E-06	1.39	1.43	0.00E+00	0.02	0.02
delta_t =	800	80.50	3.96E-06	1.38	1.45	0.00E+00	0.02	0.02
		80.75	3.94E-06	1.37	1.48	0.00E+00	0.02	0.02
		81.00	3.93E-06	1.37	1.51	0.00E+00	0.02	0.02
sink_vel (m/s) =	0.000075	81.25	3.91E-06	1.36	1.53	0.00E+00	0.02	0.02
sink_vel (m/d) =	6.5	81.50	3.89E-06	1.35	1.56	0.00E+00	0.02	0.02
		81.75	3.87E-06	1.34	1.59	0.00E+00	0.02	0.02
		82.00	3.85E-06	1.33	1.62	0.00E+00	0.02	0.02
TIME COUNT:		82.25	3.83E-06	1.32	1.64	0.00E+00	0.02	0.02
		82.50	3.81E-06	1.32	1.67	0.00E+00	0.02	0.02
t_total(s) =	93600000	82.75	3.79E-06	1.31	1.70	0.00E+00	0.02	0.02
t_total(h) =	26000.00	83.00	3.78E-06	1.30	1.72	0.00E+00	0.02	0.02
t_total(d) =	1083.33	83.25	3.76E-06	1.29	1.75	0.00E+00	0.02	0.02
t_total(yrs) =	3.0	83.50	3.74E-06	1.28	1.78	0.00E+00	0.02	0.02
		83.75	3.72E-06	1.27	1.80	0.00E+00	0.02	0.02
		84.00	3.70E-06	1.27	1.83	0.00E+00	0.02	0.02
		84.25	3.68E-06	1.26	1.86	0.00E+00	0.02	0.02
		84.50	3.66E-06	1.25	1.88	0.00E+00	0.02	0.02
		84.75	3.64E-06	1.24	1.91	0.00E+00	0.02	0.02
		85.00	3.63E-06	1.23	1.94	0.00E+00	0.02	0.02
		85.25	3.61E-06	1.22	1.96	0.00E+00	0.02	0.02
		85.50	3.59E-06	1.22	1.99	0.00E+00	0.02	0.02
		85.75	3.57E-06	1.21	2.02	0.00E+00	0.02	0.02
		86.00	3.55E-06	1.20	2.05	0.00E+00	0.02	0.02
		86.25	3.53E-06	1.19	2.07	5.45E-08	0.02	0.02
		86.50	3.51E-06	1.18	2.10	5.45E-08	0.02	0.02
		86.75	3.49E-06	1.17	2.13	5.45E-08	0.02	0.02
		87.00	3.48E-06	1.16	2.15	1.42E-07	0.02	0.02
		87.25	3.46E-06	1.15	2.18	1.42E-07	0.02	0.02
		87.50	3.44E-06	1.13	2.21	2.29E-07	0.02	0.02
		87.75	3.42E-06	1.11	2.23	3.27E-07	0.02	0.02
		88.00	3.40E-06	1.08	2.26	4.92E-07	0.02	0.02
		88.25	3.38E-06	1.05	2.29	5.74E-07	0.01	0.02
		88.50	3.36E-06	1.00	2.31	6.05E-07	0.01	0.02
		88.75	3.34E-06	0.94	2.34	6.05E-07	0.01	0.02
		89.00	3.33E-06	0.87	2.37	6.05E-07	0.01	0.02
		89.25	3.31E-06	0.79	2.39	5.74E-07	0.01	0.02
		89.50	3.29E-06	0.70	2.42	4.92E-07	0.00	0.02
		89.75	3.27E-06	0.60	2.45	2.29E-07	0.00	0.02
		90.00	3.25E-06	0.50	2.48	-2.89E-07	0.00	0.02
		90.25	3.23E-06	0.40	2.50	-2.89E-07	0.00	0.02
		90.50	3.21E-06	0.31	2.53	-4.82E-07	0.01	0.02
		90.75	3.19E-06	0.22	2.56	-5.50E-07	0.01	0.02
		91.00	3.18E-06	0.15	2.58	-7.15E-07	0.01	0.02
		91.25	3.16E-06	0.09	2.61	-7.15E-07	0.01	0.02
		91.50	3.14E-06	0.04	2.64	-7.70E-07	0.02	0.02
		91.75	3.12E-06	0.01	2.66	-7.70E-07	0.02	0.02
		92.00	3.10E-06	0.00	2.69	-8.25E-07	0.02	0.02
		92.25	3.08E-06	0.00	2.72	-8.25E-07	0.02	0.02
		92.50	3.06E-06	0.02	2.74	-8.25E-07	0.03	0.02
		92.75	3.04E-06	0.05	2.77	-8.25E-07	0.03	0.02
		93.00	3.03E-06	0.10	2.80	-8.25E-07	0.03	0.02

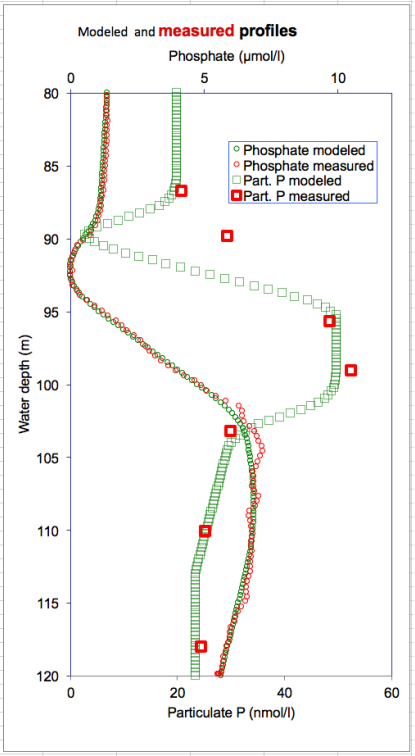

In this overall approach, the dissolved phosphate concentrations, which we measured accurately and with high vertical resolution, is the starting point of the model and the modelled values follow closely the measured concentrations. The modelled values for particulate phosphorus, which we determined with much lower resolution and accuracy, only roughly represent the measured concentrations. Principally, this problem could be addressed, e.g., by applying changing sinking velocities with depth, but unless more precise data on the distribution of particulate phosphorus are available, this would not improve our overall understanding of the system.

References

1. Weinbauer MG, Fritz I, Wenderoth DF, Höfle MG. Simultaneous extraction from bacterioplankton of total RNA and DNA suitable for quantitative structure and function analyses. Appl Environ Microbiol. 2002;68:1082-7.

2. Satinsky BM, Gifford SM, Crump BC, Moran MA. Use of internal standards for quantitative metatranscriptome and metagenome analysis. Methods Enzymol. 2013;531:237-50.

3. Stolle C, Labrenz M, Meeske C, Jürgens K. Bacterioneuston community structure in the southern Baltic Sea and its dependence on meteorological conditions. Appl Environ Microbiol 2011;77:3726–33.

4. Chevreux B, Wetter T, Suhai S. Genome sequence assembly using trace signals and additional sequence information. Computer Science and Biology: Proceedings of the German Conference on Bioinformatics (GCB). 1999;99:45-56.

5. Joshi NA, Fass JN. Sickle: A sliding-window, adaptive, quality-based trimming tool for FastQ files *[Software]* (Version 1.33) 2011 [Available from: https://github.com/najoshi/sickle.

6. Peng Y, Leung HC, Yiu SM, Chin FY. IDBA-UD: a de novo assembler for single-cell and metagenomic sequencing data with highly uneven depth. Bioinformatics. 2012;28:1420-8.

7. Hyatt D, Chen G-L, LoCascio P, Land ML, Larimer FW, Hauser LJ. Prodigal: Prokaryotic gene recognition and translation initiation site identification. BMC Bioinformatics. 2010;11:19.

8. Camacho C, Coulouris G, Avagyen V, Ma N, Papadopoulos J, Bealer K, et al. BLAST+: architecture and application. BMC Bioinformatics. 2009;10:421.

9. Temperton B, Gilbert JA, Quinn JP, McGrath JW. Novel analysis of oceanic surface water metagenomes suggests importance of polyphosphate metabolism in oligotrophic environments. PLoS ONE. 2011;6:e16499.

10. Langmead B, Trapnell C, Pop M, Salzberg SL. Ultrafast and memory-efficient alignment of short DNA sequences to the human genome. Genome Biol. 2009;10.

11. Liao Y, Smyth GK, Shi W. FeatureCounts: An efficient general purpose program for assigning sequence reads to genomic features. Bioinformatics. 2014;30:923-30.

12. Kielbasa SM, Wan R, Sato K, Horton P, Frith MC. Adaptive seeds tame genomic sequence comparison. Genome Res. 2011;21:487-93.

13. Gregg MC, Yakushev E. Surface ventilation of the Black Sea's cold intermediate layer in the middle of the western gyre. Geophys Res Lett. 2005;32:L03604.

Figure 1

Further examples for phosphorus rich particles with chains of magnetite from the suboxic zone of the Black Sea. The approximate diameter of the spherical cells (4.6 - 6.6 µm) are given below.

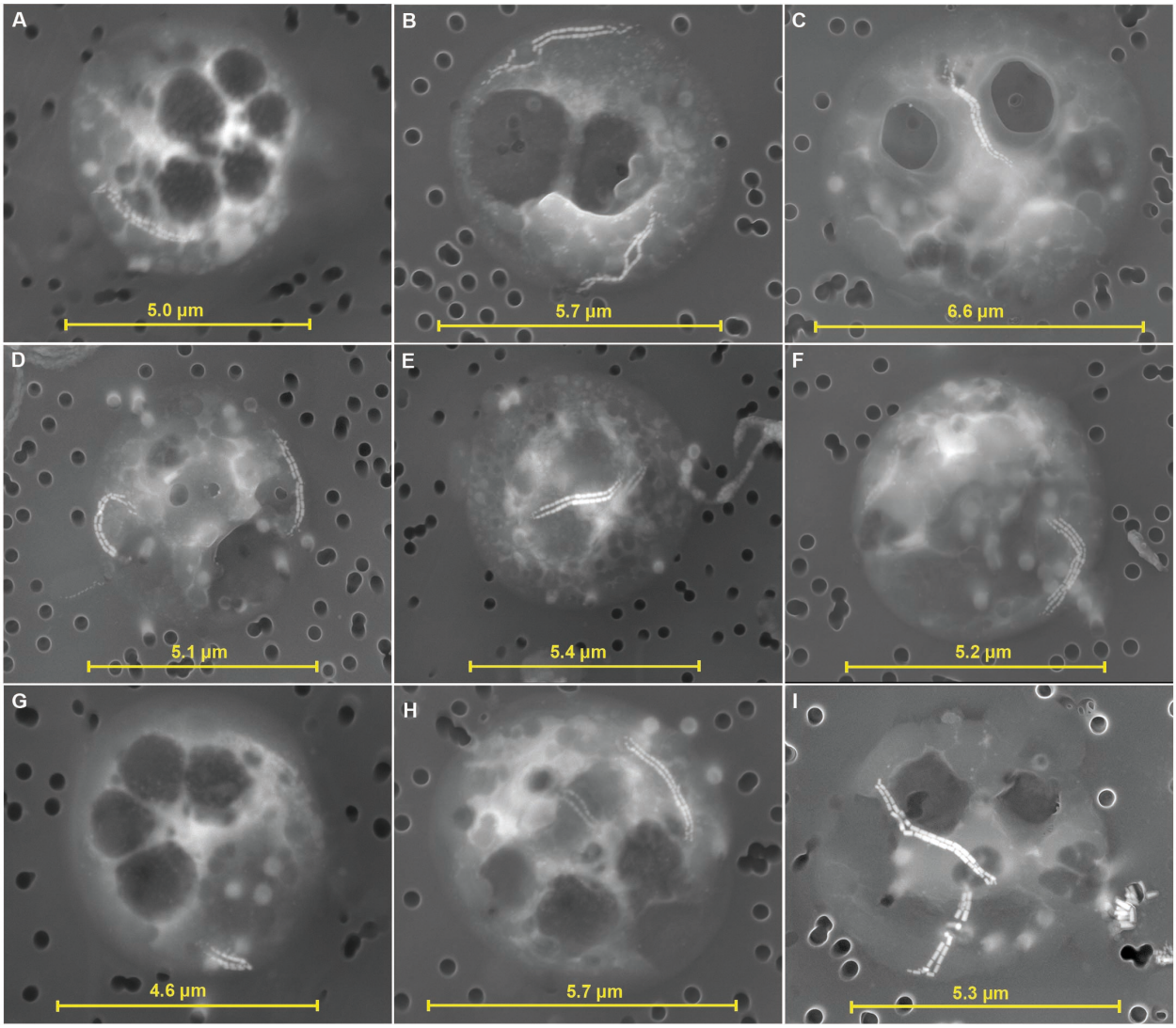

Figure 2

Identification of magnetosomes from the suboxic zone of the Black Sea by EDX analysis. (**A**) A chain of magnetosomes within a cell. (**B**) Spectrum of a magnetite crystal showing the high iron content.

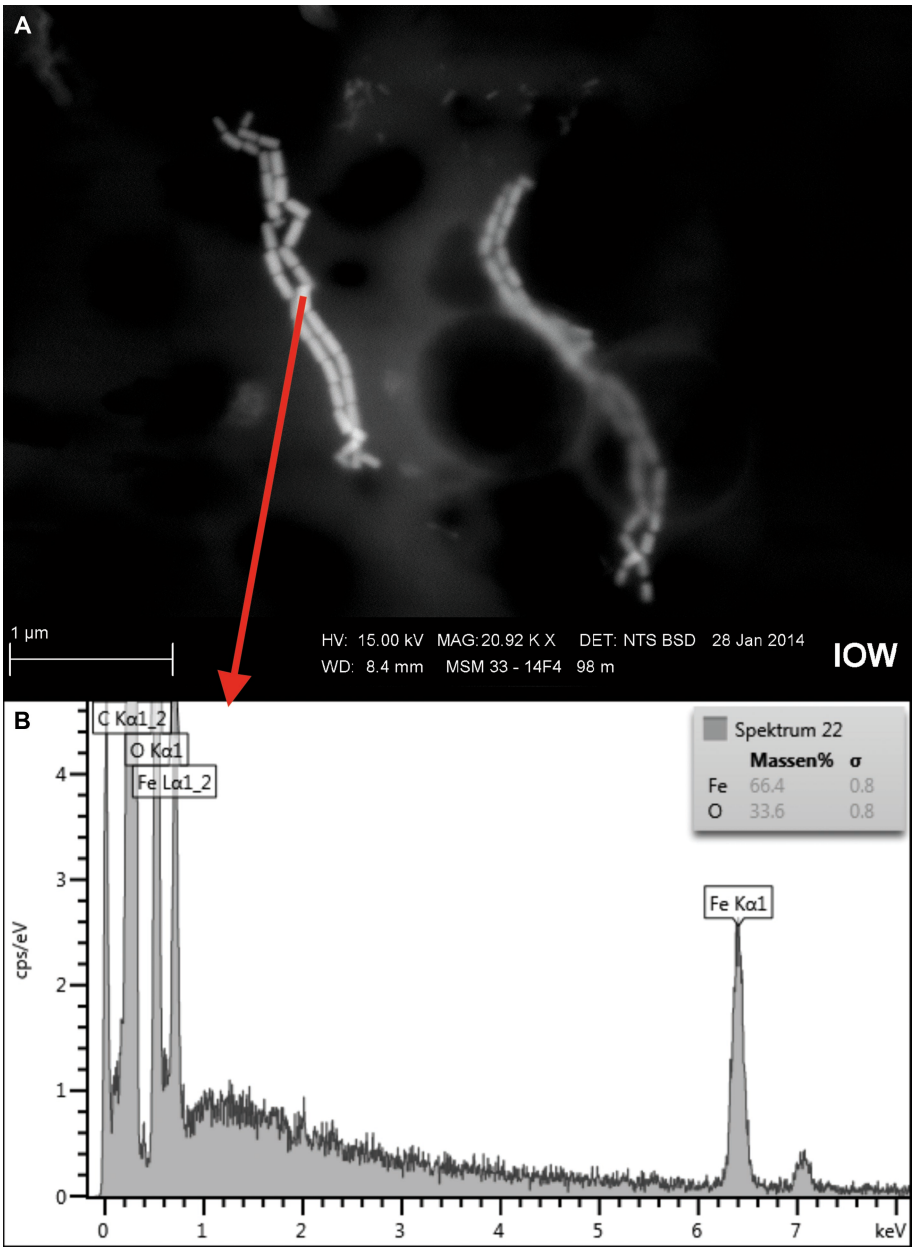

Figure 3

Chains of magnetites detected in sediment traps from the redoxcline in the Gotland Basin of the Baltic Sea. Similar chains were also observed in samples taken from the redoxcline.

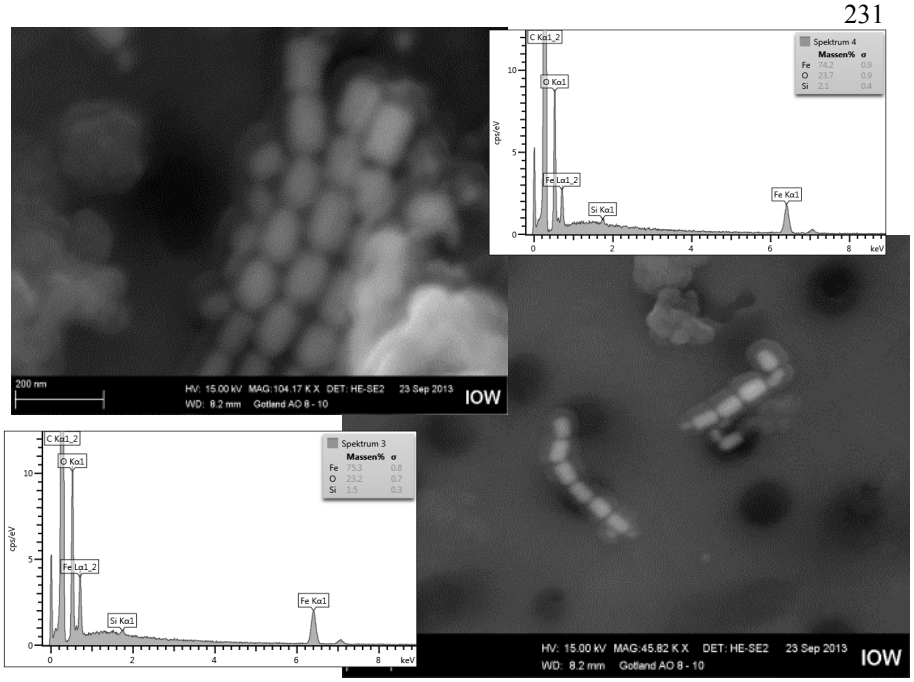

Figure 4

Example for the specific staining of large spherical cells with the probe specific for *Magnetococcus* related bacteria in samples from the Black Sea. (**A**) All microbial cells stained with 4,6-Diamidin-2-phenylindol (DAPI). (**B**) Cells hybridized with the probe specific for *Magnetococcus* related bacteria.

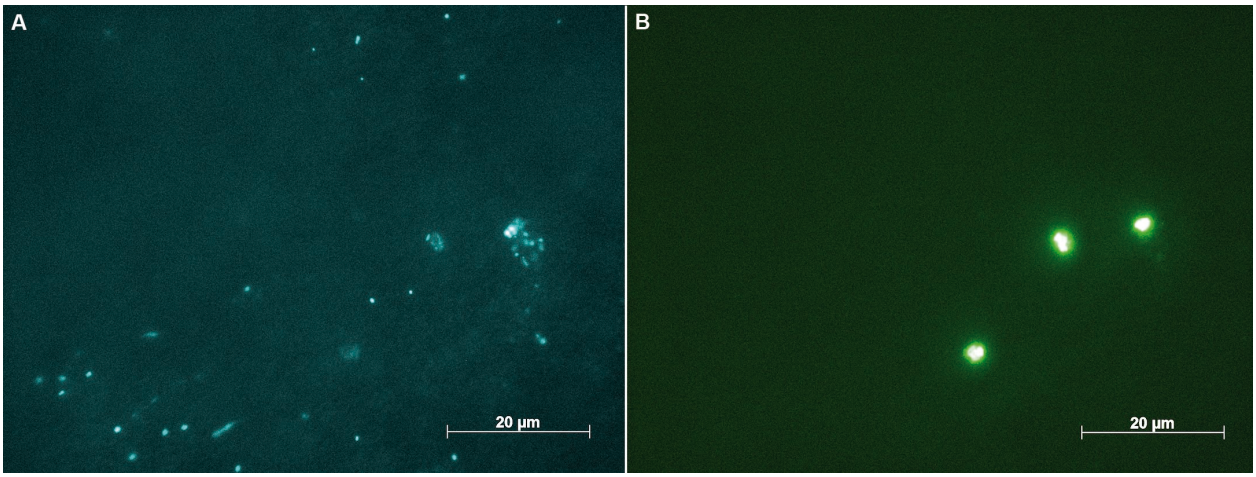

Figure 5

Maximum likelihood tree of the abdundant sequences derived from the Black Sea samples affiliated to the Magnetococcaceae and related sequences from the ARB Silva database. A core tree based on 1274 unambiguously aligned sequence positions of the full-length sequences from the database was calculated and short sequences added without changing the tree toplogy. *Magnetococcus marinus* MC-1 was set as outgroup. Original sequence definitions in the GenBank database were replaced with a consistent nomenclature including accession number, name and for the sequences from this study the number of reads detected. Bold sequences indicate the sequences with a 100% match to MaCo983. Short 16S rRNA sequences that were used for the phylogenetic analysis are deposited in the European Nucleotide Archive (ENA) under accession numbers LT960764-LT960776.

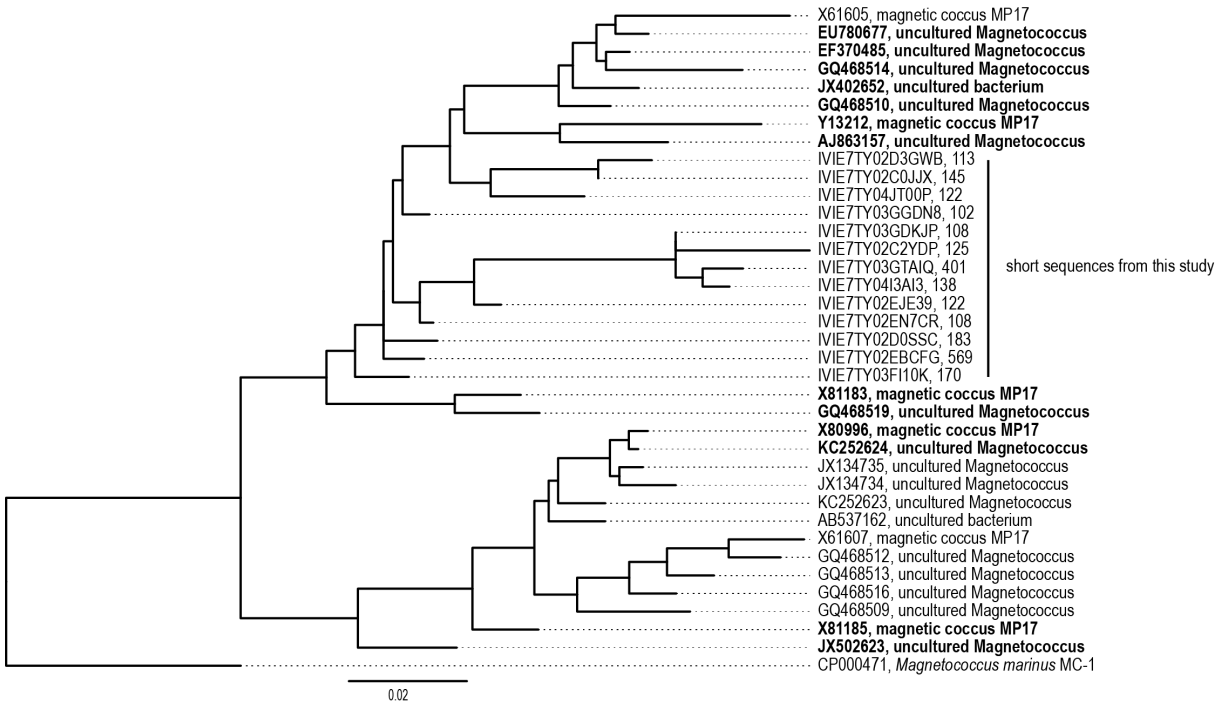

Table 1

Concentration of total dissolved phosphorus in µmol/l determined by ICP-OES and phosphate determined colorimetrically at different water depths.

Depth (m)	diss P (µM)	Phosphate (µM)
72	1.6	1.3
77	1.6	1.4
87	1.3	1.3
90	0.9	0.7
92	0.2	0.0
96	2.2	1.7
99	4.6	4.0
103	6.7	6.9

Table 2

Relative abundance of particles rich in iron (>15%), rich in manganese (>10%), and rich in P (>20%) in % of all particles.

Depth (m)	Fe-rich (%)	Mn-rich (%)	P-rich(%)
72	3.3	57.7	0.0
87	6.8	41.9	1.1
90	3.3	60.3	0.2
95	17.8	29.3	13.5
100	28.6	6.8	2.9
103	25.1	40.3	18.1
110	34.2	0.7	0.2
118	15.8	0.2	0.1

Table 3

Concentration of phosphorus, iron and manganese in the particulate pool determined by ICP-OES in nmol/l.

Depth (m)	P_{part} (nM)	Fe_{part} (nM)	Mn_{part} (nM)
72	21.8	34.3	45.2
87	20.8	33.4	28.5
90	29.4	25.3	47.7
95	48.6	28.6	6.7
100	52.6	31,8	5.3
103	29.9	24.5	15.6
110	25.2	22.7	5.1
118	24.4	21.1	2.0